Understanding the Contribution of Terrestrial Radiation Sources to Quantum Devices Error Rate

Gioele Casagranda, Marzio Vallero, Flavio Vella, and Paolo Rech

***Abstract*—Quantum Computing (QC), despite being a highly promising computational paradigm, suffers from an incredibly high radiation sensitivity. Recent discoveries highlighted that the impact of a particle in the quantum bit (qubit) is tens of thousands times more likely to induce a fault compared to traditional CMOS devices. Moreover, the deposited charge quickly diffuses in the substrate affecting multiple qubits, inducing faults that can persist for hundreds of seconds.**

In this paper, we aim to better understand the effect of different radiation sources and mechanisms of energy propagation on quantum devices. We present data from the simulation of more than 18 billion particle interactions. Through GEANT4 simulations, we compare the effect of neutrons, alpha particles, muons, and gamma rays in a quantum device. We combine non-equilibrium generation probability with natural flux to identify the most harmful radiation source for qubits. We found that muons are, by far, the more likely cause of faults in qubits. Moreover, through G4CMP simulations, we track the energy propagation within the substrate. We show that even particle hits far from the qubit can lead to energy transmission to the superconductor, also pointing out that this mechanism is 1,000 more likely than a direct energy deposition on the qubit. In addition, we show that the time persistency of secondary particles in the substrate is in the order of O(100 μs). Finally, we look at particle impacts on a four-qubit device to show that with a common layout, multiple-qubit are likely to be corrupted.

I. Introduction

Over the past few years, the bound to the miniaturisation of classical chips, in conjunction with increasing investments in the field, has elevated Quantum Computing (QC) to a compelling technological solution to solve an always larger class of problems. The key feature of QC is to exploit quantum properties of matter (superposition and entanglement) as a computing resource rather than as an interference. Despite the intense dedication of the community, a crucial issue is still acting as a bottleneck for the large-scale adoption of QC: every existing implementation suffers from reliability problems. The focus has been oriented on the study of the intrinsic decoherence problem, called noise, which already led to (extremely expensive) working strategies of suppression, namely surface codes, and neglecting other threats, such as radiation [1].

Preliminary studies highlighted that quantum devices, circuits and error correction subroutines are particularly susceptible to radiation [2]–[8]. In spite of the apparent layout similarities between CMOS transistors and superconducting qubits, the radiation sensitivity of the latter is orders of magnitude higher than that of the former and presents a peculiar behaviour yet to be fully understood. The available observations show that the occurrence rate of radiation events in quantum chips is extremely high compared to the most modern supercomputers one [2], [9]. The reason is rooted in the nature of quantum bits (qubits): even a minor energy deposition can induce non-equilibrium conditions in the quantum states. Conversely to CMOS transistors, then, there is no activation energy threshold for the change of state of the qubit [10]. This also implies that particles hitting the substrate at far distances from the qubit's active region can still modify its state. Additionally, the impact of one single particle is likely to spread in the Silicon substrate affecting multiple qubits at once [2]. Most concerningly, such particle strikes can invalidate the functioning of qubits for several seconds rather than just nanoseconds [11].

One of the crucial matters we target in this paper is to determine which particles represent the most relevant source of error in quantum devices, according to their origin and energy. Moreover, we investigate the possible reasons for the peculiar fault persistence and fault spread of radiation-induced faults in quantum devices. For classical CMOS devices, neutrons represent the most problematic cause of transient faults on Earth, due to their energy spectrum and interaction properties [12]. Given that the concept of critical charge is not applicable to quantum devices, even light (and abundant) particles, such as muons (almost unharmful for CMOS), have a chance of disrupting the quantum state of a qubit [4].

We focus on the study of a prototypical Xmon (based on transmon technology) qubit and the IBM SQUID loop [13]. To evaluate the contribution of different particles of different energies to their error rates, we discuss a comparison, based on GEANT4 toolkit extensive simulations, between the effects induced by (a) cosmic neutrons of $1 - 100$ MeV, (b) muons of $0.1 - 10$ GeV, (c) gamma rays of $0.1 - 2$ MeV and (d) alpha particles $1 - 10$ MeV present in the intrinsic radioactivity of materials. For each particle, we (i) discuss the energy deposition mechanism, (ii) show the energy deposition probability distribution, and (iii) calculate the cross-section.

This work was supported partly by the Italian Ministry for University and Research (MUR) through the Departments of Excellence 2023-27 program under Grant L.232/2016 awarded to the Department of Industrial Engineering, and partly by a CINECA award under the ISCRA initiative, by providing high-performance computing resources and support within the Q-CORE project.

This project has been supported by Q@TN, the joint lab between the University of Trento, FBK- Fondazione Bruno Kessler, INFN-National Institute for Nuclear Physics and CNR-National Research Council with financial resources from PAT (Provincia Autonoma di Trento).

Gioele Casagranda, Marzio Vallero and Flavio Vella are with the Department of Information Engineering and Computer Science of the University of Trento, Italy (e-mail: gioele.casagranda@unitn.it, marzio.vallero@unitn.it, flavio.vella@unitn.it).

Paolo Rech is with the Department of Industrial Engineering of the University of Trento, Italy (e-mail: paolo.rech@unitn.it).

Then, (iv) we combine the integral contribution of each particle to the quantum device error rate and (v) normalize it by the expected flux at sea level. Our experiments show that muons are the most likely source of faults for quantum devices. Gammas and alphas contribute significantly to the error rate, however gammas can be easily shielded (even by the qubit cooling system itself), whilst alphas can be reduced by making use of purified materials. The contribution from neutrons is much lower than other sources. We further investigate the behaviour of a qubit under radiation employing the G4CMP toolkit [14] to simulate the creation and propagation of energy carriers, which are phonons and electron-hole pairs. We look at their temporal persistence and spatial diffusion within the substrate before being absorbed by the superconductor, or before escaping the system. The observations show that energy spreads throughout the entire volume of the substrate for a timespan of O($100\mu s$). Overall, we present data from the interactions of more than 18 billion generated particles.

The remainder of the paper is structured as follows. Section II serves as a background on quantum computing and quantum devices. In Section III, we present our experimental setup and methodology. Section IV presents the results for the energy deposition of different sources on the SQUID loop. The analysis continues in Section V with data on energy deposition in qubits, energy propagation through secondary production, and an examination of the effects of energy deposition on a substrate containing multiple qubits. Finally, Section VI concludes the paper.

II. Background

In this Section, we provide background material on quantum computing, discuss the reliability issue in qubits, and summarise the latest discoveries in radiation-induced effects on quantum devices.

A. Quantum Computing essentials

In a classical computer, CMOS transistors state encodes the binary digit 0 *or* 1. Quantum computer architecture does not rely on this binary representation of information: the unit is represented by the quantum bit (qubit). A qubit can be physically modelled as a 2-level quantum system that logically represents the linear combinations of two different states: $|\Psi\rangle = \alpha|0\rangle + \beta|1\rangle$, where α and β are complex numbers that represent the respective amplitudes. Similarly to classical computing, the two states are identified with $\{|0\rangle, |1\rangle\}$. In general, a qubit is a quantum *superposition* of the two states: it does not exist as a single deterministic value. A *measurement* is necessary to read the information in a qubit, whose outcome is either $|0\rangle$ or $|1\rangle$ with the probability given by the squared factors α^2 and β^2. The measurement outcome can never be deterministically predicted prior to the collapse of the wave function, which only happens when the system is measured. A full understanding of these mechanisms is beyond the purpose of this paper, but one could observe that, given the above description, the qubit is nothing else than a vector in a 3D space spanned by the states $|0\rangle$ and $|1\rangle$ and of unitary length (due to the normalisation $1 = \alpha^2 + \beta^2$). From a practical perspective, qubits can be implemented in different ways among which there are atomic orbitals, trapped ions and, most commonly, superconducting circuits. The latter represents the cutting-edge qubit design, for which many sub-categories of systems have been developed. The most reliable and promising one is the transmon, whose functioning is based on the tunnelling of Cooper pairs through one or more Josephson junctions. The devices are made of a silicon substrate and an operating part of superconducting aluminium kept at $\sim 10mK$. The core of the implementation of a transmon is the SQUID (Superconducting Quantum Interference Device), where the Josephson junctions are located (see Section III for details) [15].

B. Quantum Computing reliability

A qubit, as a physical system, is intrinsically unstable. In general, it is affected by two different decay channels. A spin-lattice mechanism can be identified, accounting for the intrinsic interactions and associated with the *decoherence time T1*. Alongside that, external couplings with the environment take the name of *spin-spin relaxation processes*, which are bound to the time T2 [16]. These factors represent the ultimate temporal limit for quantum information retention. Both these time scales have been rising in the last years thanks to technological improvements: in a couple of decades their values went from 1 ns to 100 μs.

Lately, both researchers and industries put effort into facing the problem of reliability at a logical level, and Quantum Error Correction (QEC) mechanisms have been developed. The idea is to make use of a larger number of *physical* qubits (10s to 100s or even 1000s) to control the correct functioning of a small bunch of fault-tolerant *logical* qubits through specific coding. These solutions are extremely costly, both resource and cost-wise because they introduce qubit overheads of more than 20 times [17]. Unfortunately, transient radiation-induced faults cannot be efficiently dealt with using current QEC mechanisms [8].

C. Radiation-induced fault model in qubits

Transient radiation-induced faults represent an urgent matter for quantum devices that requires a prompt solution and deserves great attention. The inner workings of transmon qubits are based on controlling the flux of Cooper pairs under specific conditions. Cooper pairs have a binding energy of 10^{-3} eV, and breaking even one of them can alter the whole qubit state, triggering non-equilibrium conditions that may lead to quantum information loss. The amount of energy required to break a Cooper pair is extremely small when compared to the critical charge of CMOS devices. There is no chance for a quantum computer to become sufficiently fault tolerant solely with the aid of shielding measures (existing devices are covered by metal shells and put in caves to prevent the interaction of lighter particles) [4], [18], [19]. These solutions are neither practical nor scaleable. There is then an urgent need to understand which processes are affecting quantum devices and why they induce the effects that we observe.

The literature offers an analysis of the impact of neutrons on SQUID loop [11], cumulative studies of the effects on qubits

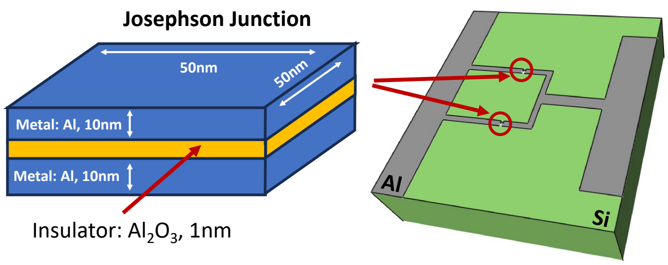

Fig. 1: SQUID layout. The aluminium superconducting loop (grey) is the sensitive volume of the experiments together with the Josephson junctions.

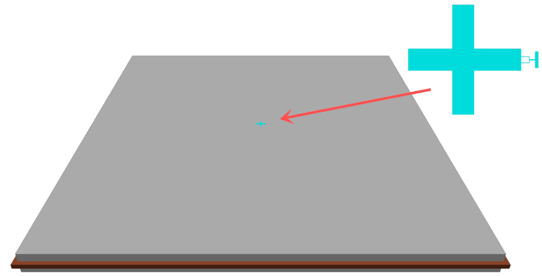

Fig. 2: Qubit layout. In grey the substrate, in cyan the superconducting layers and in brown the copper frame.

[3], [20], and field test data on real quantum chips [2]. The interesting, yet worrying, results obtained so far highlighted that (a) even light particles can deposit sufficient energy to influence a qubit state; (b) faults can persist for up to hundreds of seconds; (c) multiple qubits are likely to be affected by one single particle interaction. The goal of our paper is to bridge the gaps in the literature by understanding the harm posed by different sources of radiation.

III. GEANT4 Simulations

In this section, we detail the layout of the quantum device we test, the radiation sources, and the GEANT4 settings.

A. Quantum devices layouts

We study two different setups to provide a complete analysis of the radiation effects on superconducting qubits. Their structure can be outlined as a semiconductor wafer (*substrate*) with multiple superconducting films attached to its top surface. The latter represents the working parts of a quantum computer, taking the role of memories and computation units. Multiple structural combinations are possible, stemming in different categories. We specifically analyse an Xmon qubit, which inherits its characteristics from the class of transmon qubits [15]. This kind of qubit is made of a cross capacitively coupled at its extremes with an XY control line, a readout line and a bus line, and it is inductively coupled to a Z control line [21]. The inductive coupling part of the device takes the name of SQUID (Superconducting Quantum Interference Device) loop and represents the device's core component. It is made of a loop interrupted by two Josephson junctions symmetrically placed, the key elements for qubit operation. A Josephson junction consists of a three-layer structure, where an insulator is interposed between two thin layers of superconducting material [22], [23]. The small insulating gap (O(1 nm)) acts as a barrier for the Cooper pairs, that can only be crossed via quantum tunnelling. This behaviour, induced by the coherent interference of the Cooper pair wavefunctions at the two ends of the junction, shows a nonlinear relation to the voltage applied and makes the junction a non-linear inductor [24], [25]. An alteration of the density of Cooper pairs at the ends of the Josephson junctions leads to a loss of information, and thus to a disruption of computation. We look at all the energy deposition in these positions, which means on the cross and the SQUID loop.

1) SQUID experiments: SQUIDs also exist as independent elements, acting as extremely sensitive magnetometers which can be used to measure weak magnetic fields. The SQUID we tested (Figure 1) is based on the Qiskit Metal documentation by IBM [13] and consists of a Silicon substrate of 10 μm thickness and a surface of 40 μm by 37 μm. The superconducting loop is made of Aluminum and is 50 nm thick. The Josephson junctions are built with an Aluminium oxide insulator (Al_2O_3) 1 nm thick, interposed by two Aluminum layers 10 nm thick.

We modelled the SQUID with CAD and exported it to GEANT4 as a triangularly tessellated solid. Within GEANT4, the device is placed in a world structure filled with an extremely rare gas, simulating theintergalactic vacuum.

2) Qubit Experiments: The second setup taken into account consists of a larger (8 mm by 7.4 mm) and thicker (380 μ m) Silicon substrate, chosen to resemble the setups of other works [26], [27] and typical implementations. The 50 nm-thick superconducting layer is limited to sensible areas for Cooper-pair breaking: a plus-shaped area (called "island"), whose arms are 100 μm long and 40 μm large, and the SQUID loop, which has the same sizes previously described (Figure 2). The materials chosen are Silicon for the substrate and Aluminum for the superconductor which are in accordance with existing qubit implementations. The device is embedded in a Cu frame that simulates its possible placement within a working quantum computer.

B. Radiation Sources and GEANT4 settings

The spectrum of terrestrial particles that could potentially affect the state of a quantum device ranges from neutrons and alphas to light and fast gamma rays and muons. We aim at understanding which kinds of particles contribute more to the quantum device error rate, considering the particle interaction and average flux. GEANT4 can account for a wide range of interaction processes and different mechanisms to excite the target material. We developed a custom physics list starting from the *QGSP_BIC_EM* physics list, which resolves both ionising, indirect ionising (for neutral particles) and non-ionising processes. In addition to that, thanks to G4CMP toolkit, we extended our analysis to a wider range of physical phenomenons by adding low-energy physics processes. These involve the creation and recombination of e^-/h^+ pairs, the generation of phonons, the downconversion of phonons to low-energy ballistic phonons, and the emission of Luke phonons.

1) SQUID experiments: The particle source is placed in proximity to the top surface of the SQUID, at a distance on the order of the involved particles. This ensures that particles get created before they interact with matter. The source is a plane surface of the same size as the SQUID section and particles are radiated isotropically in the 2π solid angle facing the SQUID.

We perform individual simulations for each particle species, firing 10^8 particles for every chosen energy. The **neutron** flux at sea level shows three peaks, one in the range of the thermal energies (0.1-1 eV), one around 1 MeV and one at 100 MeV [28]. The thermal peak is not relevant for the quantum chips [11], therefore we test neutrons with 1 MeV, 100 MeV and where the flux has a minimum, at 10 MeV. **Muons** spectrum is increasingly smooth from 100 MeV to 10 GeV [28], therefore we test these two energy values and the middle (logarithmically) energy of 1 GeV for both negative (μ^-) and positive (μ^+) muons. Regarding **gamma rays**, their spectrum has a cutoff around 2.6 MeV [4]; we test values of energies of 100 keV, 1 MeV and 2 MeV. Finally, for what concerns **alpha particles**, we need to consider that the spectrum is heavily source-dependent, we then perform the simulations for a wider number of typical energies: 1,3,5,7,10 MeV. In total, we present data from 17 different physical simulations on the SQUID.

2) Qubit(s) experiments: From the analysis of the SQUID data, it emerges that the impact angle does not significantly affect the results. As such, this set of experiments simulates impacts of particles impinging perpendicularly to the device. We performed three distinct classes of experiments with the qubit. As a first analysis, we replicated the energy deposition measurements done for the SQUID, by firing the same particles with the same energy as in the previous experiment. To improve the statistics, for each issue, we injected 10^9 particles from a surface 5 mm x 5 mm centred on the device.

We then switched on the low-energy physics processes, in order to account for energy propagation. In this case, the analysis has been limited to smaller samples due to the high computational intensity, testing different sample sizes according to the type of particle (details provided in Section V). Every energy deposition in the substrate triggers the creation of e^-/h^+ pairs which subsequently can either recombine or generate a small amount of highly energetic phonons. Within a short time, these downconvert to ballistic (lower energy) phonons that eventually diffuse in the substrate. The low temperature of the systems theoretically lets the phonons persist in the substrate for extremely long periods of time. The only escape routes for these phonons are the superconductor and the Copper frame. We modelled the collision with both boundaries according to real measurements [29] and theoretical calculations for wave propagation [26]. Finally, we made a weighted average of the results considering the density of the phonons in our simulations (either transversal or longitudinal) to get the following phonon absorption probabilities: $P_{Cu} = 0.739$, $P_{Al} = 0.802$. If the particle is not absorbed, the surface behaves as a boundary, reflecting the phonon. On the contrary, electrons and holes are always absorbed by whichever surface they hit.

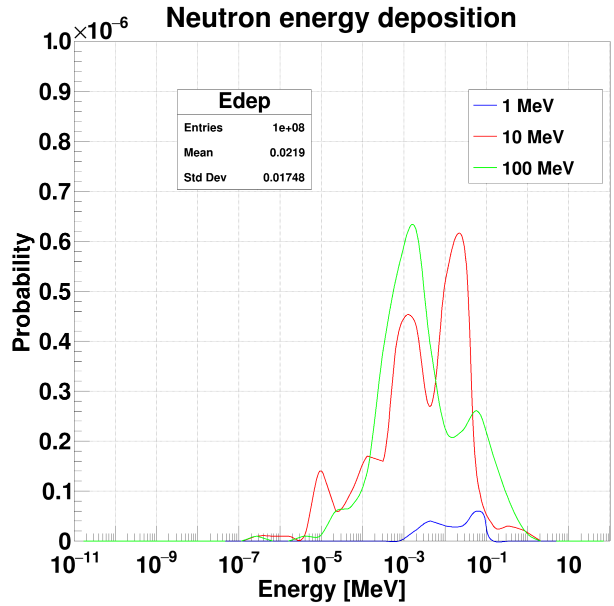

Fig. 3: Probability for 1 MeV (blue), 10 MeV (red), and 100 MeV (green) neutrons to deposit energy on the SQUID.

As a last experiment, we investigate the deposition of energy on a substrate hosting multiple qubits. Four qubits are placed equidistantly from each other, with a separation of 4 mm from the closest neighbours, and 2.5 mm from the outer edge of the Si substrate. For reasons that will emerge clearly in the following Section, the chosen particle source is a positive muon beam at 10 GeV, focused on a single point of the device. We perform three sub-experiments injecting 2,500 particles, that only differ for the impact position: in the centre of the substrate (equally distant from all the qubits), in the midpoint between two qubits, and directly in the centre of a qubit.

IV. Results for the SQUID Experiments

In this section, we present the analysis of the SQUID simulations. For each particle, we test the most representative energies, discuss the energy deposition mechanism, and measure the probability of energy deposition from 10^8 interactions. We then measure the cross-section by counting the events that deposit sufficient energy to break a Cooper pair, trigger non-equilibrium and thus corrupt the qubit state. Results are then combined with the natural flux.

A. Neutrons

Neutrons are the main concern for classical CMOS transistors and therefore the first natural candidate to investigate. Since they are chargeless particles, their interaction rate with matter is not high. Only short-distance forces can be involved in the coupling with the Aluminium lattice and the Al_2O_3 in the Josephson junction. The observable interactions are elastic and inelastic scattering and capture processes. The main contribution is given by the former channel since it can initialise a cascade process where the PKA (primary knock-on atom) induces the ionisation of the lattice [11].

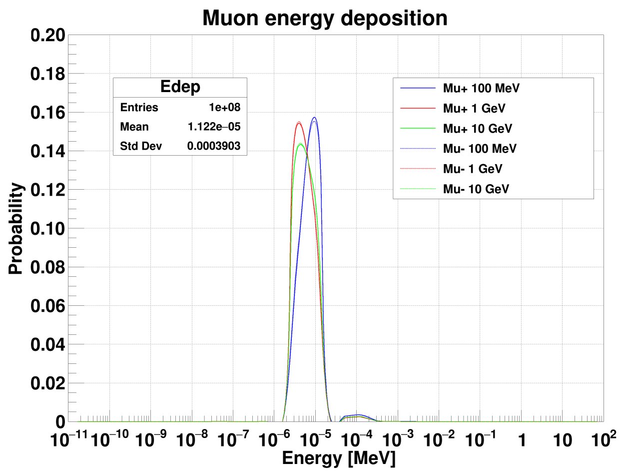

Fig. 4: Energy deposition probability for six packets of 10^8 muons, at energies 100 MeV (blue), 1 GeV (red), and 10 GeV (green). The solid ($\mu+$) and dashed line ($\mu-$) overlaps.

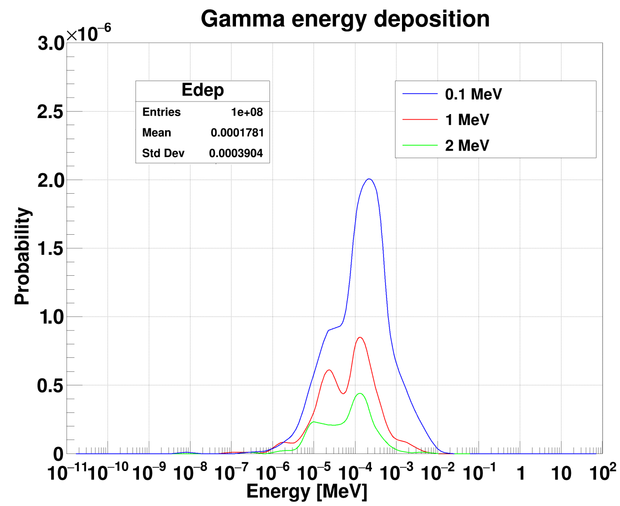

Fig. 5: Energy deposition probability for three packets of 10^8 photons, at energies 100 keV (blue), 1 MeV (red), and 2 GeV (green).

In Figure 3 we show the results for three bunches of energies (1, 10, 100 MeV). This choice is justified by the spectrum at the sea level [28], which shows two peaks at 1 and 100 MeV. Thermal neutrons, whilst also being abundant, are excluded from our analysis since they have a negligible effect on quantum devices [11].

Figure 3 shows the probability for a neutron to deposit a certain energy. The values on the vertical axis are normalised by the number of total impinging particles, thus the plot represents the probability of a particle depositing a certain energy. The probabilities are observed to be: $P_{(1MeV)} = 1.80 \times 10^{-7}$, $P_{(10MeV)} = 3.14 \times 10^{-6}$, $P_{(100MeV)} = 3.22 \times 10^{-6}$. Neutrons at 1 Mev are less likely to deposit energy on the device, whereas at energies $>$ 10 MeV the number of interactions is not energy dependent. The peaks of the distributions are centred on 1-10 keV, indicating that the events are probably a result of indirect ionisation. The distribution shape and the number of counts agree with previous work [11].

The key point illustrated in Figure 3 is that the energy released by neutrons is significantly higher than the energy required to break the binding of a Cooper pair (a few meV) [10]. Neutrons then interfere with the superconductor, potentially altering the qubit state. We calculate the cross-section of the upset event in a SQUID, following the definitions for classical devices. The flux of particles is given by $\Phi = N_n/Area_{SQUID} = 6.76 \times 10^{12} n/cm^2$. Assuming that any energy deposition greater than the Cooper pair binding energy triggers a fault, we can take the number of neutrons that deposit energy higher than meV and divide it by Φ. This gives us the following cross sections: $\sigma^N_{1MeV} = 2.66 \times 10^{-12} cm^2 \mid \sigma^N_{10MeV} = 4.64 \times 10^{-11} cm^2 \mid \sigma^N_{100MeV} = 4.76 \times 10^{-11} cm^2$.

B. Muons

Muons are very abundant particles in the cosmic ray flux at sea level. A muon is a lepton, 10 times lighter than a neutron. The flux of cosmic muons is a mixture of positively (μ^+) and negatively (μ^-) charged particles, almost equally distributed. We simulated both of them with energies that sample the natural flux: 100 MeV, 1 GeV, and 10 GeV.

Given the presence of a charge, the interaction with the Aluminium and Al_2O_3 target takes place via the electromagnetic force, which is a long-distance interaction. The energy is deposited through two different channels. The predominant one is ionisation, which is a continuous process and suggests that most muons will interact with the device. Another mechanism of interaction is *Bremsstrahlung*, i.e., the deflection of a light and charged particle with an associated release of gamma radiation. This process is discrete and less significant.

In Figure 4 we show the probability for a muon hitting the SQUID loop to release energy on the latter. Firstly, it can be noticed that the positive/negative charge of the particle does not affect the behaviour either qualitatively or quantitatively. The interaction probabilities for the different beams are: $P_{(100MeV)} = 0.257$, $P_{(1GeV)} = 0.273$, $P_{(10GeV)} = 0.270$ for both $\mu+$ and $\mu-$. These interaction rates are compatible with the nature of the interaction and highlight that almost all the muons passing through the aluminium or the Josephson junction release some energy. This is because the superconducting film covers approximately 30 % of the substrate. The amount of energy deposition for each event is in the order of $O(1-10eV)$ and does not depend on the initial energy charge. This value is much lower than the neutron one, but, while too low to induce a fault in most CMOS technologies, it is still sufficient to break a Cooper pair and thus modify the qubit state. The value of energy depositions higher than the Cooper pair binding energy lets us to compute the cross-section for muons interactions: $\sigma^{\mu}_{100MeV} = 3.80 \times 10^{-6} cm^2 \mid \sigma^{\mu}_{1GeV} = 4.04 \times 10^{-6} cm^2 \mid \sigma^{\mu}_{10GeV} = 3.99 \times 10^{-6}$.

C. Gamma rays

Gamma rays are massless and chargeless and are mostly produced by decay processes. The interaction with the SQUID

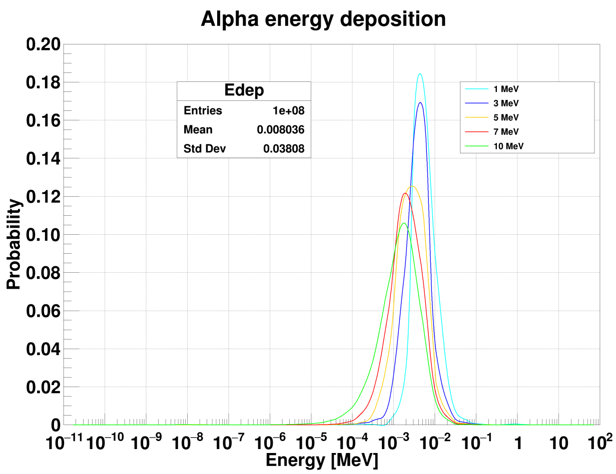

Fig. 6: Energy deposition probability for six packets of 10^8 alpha particles, at energies 1 MeV (cyan), 3 MeV (blue), 5 MeV (orange), 7 MeV (red) and 10 MeV (green).

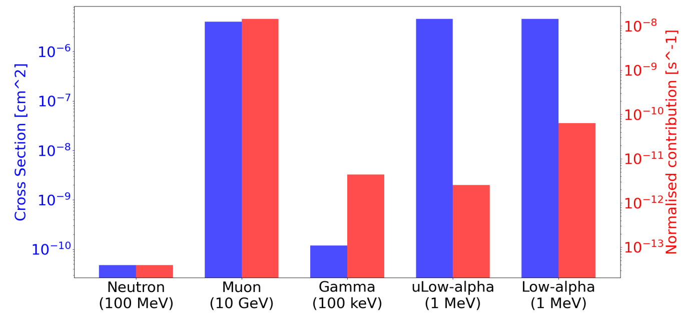

Fig. 7: Different particles contribution. The left axis shows the cross-section (blue) and the right one is the cross-section multiplied by the flux of that particle at sea level (red).

occurs via photoelectric effect and Compton scattering, which are probabilistic and not continuous events. The excited electrons can then ionise the lattice of the target, inducing indirect ionisation. Given a cutoff at 2.6 MeV in the gamma spectrum [4], we sample it by testing three beams of particles at energies 100 keV, 1 MeV and 2 MeV.

In Figure 5, we show the probability for an impinging photon to deposit a certain energy on the device. We infer that the total probabilities of releasing energies are: $P_{100\text{keV}} = 8.07 \times 10^{-6}$, $P_{1\text{MeV}} = 3.10 \times 10^{-6}$, $P_{2\text{GeV}} = 1.44 \times 10^{-6}$. The distributions for different energies share the same shape: they show a peak on the deposition of energies of 100 eV and a lower plateau down to 10 eV. The results are compatible with the ones for the other particles, with less energy deposition than neutrons and a comparable interaction rate. As expected, the latter is lower than that of muons, but the peak is shifted towards higher energy values. The released energy is always larger than the strength of Cooper pair binding, so every deposition can lead to a modification of the qubit state. The cross-sections for gamma-induced events are: $\sigma^{\gamma}_{100keV} = 1.19 \times 10^{-10} cm^2 \mid \sigma^{\gamma}_{1MeV} = 4.53 \times 10^{-11} cm^2 \mid \sigma^{\gamma}_{2MeV} = 2.13 \times 10^{-11} cm^2$.

D. Alpha particles

Alpha particles are one of the main products of nuclear reactions. They present a 2+ charge and thus interact electromagnetically as muons but, conversely to muons, alphas are typically slowed down and brought to a halt in the target. The spectrum of alpha particles is strongly correlated to their source. In general, most materials release nuclei with energies in the MeV order, so we test alphas of E={1,3,5,7,10} MeV [30].

Figure 6 shows the probability that an alpha particle deposits in the SQUID the energy values indicated on the x-axis. Integrating the curve, we notice that the total probability of interaction is the same for all particle energies (P=0.31). Considering that the surface of the Aluminium and the Al_2O_3 occupies about 30% of the SQUID surface, it means that all the alpha particles that hit the sensitive volume deposit energy.

The shape of the distribution shows a clear energy dependence. As the incident alphas get more energetic, the peak position decreases and moves towards lower energies. The value of the energy deposited is in the range $\sim 1 - 10$ eV. Coherently with our expectations, the interaction rate is close to 100% and the energy deposition is high (similarly to neutrons).

Alpha particles also deposit way larger energies than the ones needed to induce decoherence of the qubit. The cross-sections for alphas are: $\sigma^{\alpha}_{1MeV} = 4.60 \times 10^{-6} cm^2 \mid \sigma^{\alpha}_{>1MeV} = 4.59 \times 10^{-6} cm^2$.

E. Combined analysis

In Figure 7 we summarise the outcomes of our simulations. We plot in blue, for each particle, the worst-case cross-section amongst the different energies. Charged particles interact with the SQUID in a continuous way, while neutral particle interactions are ruled by probabilistic events and their cross-section is around 4 orders of magnitude smaller. The cross-section values are extremely high compared to modern CMOS devices and attest that there is almost no chance for a quantum state to avoid corruption from single particle hits.

In order to account for the probability for a particle to hit the SQUID, in Figure 7 we plot in red the relative contribution, by multiplying the cross-section and the typical flux at sea level [28]. The interpretation is that muons, being extremely interacting and abundant particles, currently represent the biggest harm for quantum devices. Gamma rays have an even higher flux at sea level, making them them an important source of error despite their tendency to have a lower interaction capability. For what concerns alpha particles, modern technologies give room to the development of materials which emit ultra-low amounts of them. Nevertheless, the innermost layers of materials can still be the cause of issues for the qubit. At last, neutrons, the biggest concern for CMOS, provide the least significant contribution to the total energy deposition process. This does not mean that neutrons are not affecting the coherence of qubits. Rather, it describes the scale of the phenomenon that we are dealing with and helps convey the magnitude of the threat that radiation poses to quantum computer reliability and the urgent need for a solution.

V. Results for the Qubit(s) Experiments

In this Section, we go over the results of the analysis of a full qubit placed on a Silicon substrate. Three sub-experiments have been conducted: (1) we replicate the energy deposition experiments performed for the SQUID to see if there is any layout-related difference; (2) we focus on the worst radiation source for quantum devices (the most energetic muons) and analyse secondary production in the substrate (similar results can be obtained for different energies and particles); (3) we perform a study of the energy deposition on a substrate hosting 4 qubits in order to understand what is the likelihood for one single particle to corrupt multiple qubits. The choice of muon as a testing particle directly derives from the results of the previous section. We have shown that muons are the most harmful particles, so analysing their effect would present the worst picture possible of the qubit reliability. Moreover, since the interaction rate of muons is really high, almost all the muons impacting the device are likely to give rise to large cascades of secondary phonons in the Silicon substrate and eventually create a large set of data to analyse. To keep track of possible differences in the response of the qubit to other types of particle impacts, we actually performed a parallel analysis for every species. In order not to be redundant, we limit the presentation to a summary at the end of the respective subsection.

A. Energy deposition

In Figure 8 we show the energy deposition probability of a muon impacting the qubit (substrate and superconducting loop), analogously to what has been discussed for the SQUID loop. We plot the result of the interaction of the particles both with the substrate (main figure) and with the superconductor (visible in the embedded figure). It is evident that most of the energy of the impinging particles is absorbed by the system through the substrate. Not only a deposition on the substrate is extremely more likely since the size of the superconducting loop is orders of magnitude smaller, but also the typical energy released in the substrate is several orders of magnitudes larger. This outcome is expected, considering the mass and the thickness of the latter compared to the thin Aluminum film. It is also the motor for the following analysis of the energy propagation mechanisms within the substrate. Nonetheless, the absorption on the superconductor is not null and its relevance rises considering that a hit on the superconductor is directly inducing Cooper pairs braking events.

As discussed in the previous Sections, we also conducted the same experiment for the other particle species obtaining very similar outcomes (not shown for lack of space): the absorption probability for the substrate is shifted to higher energies and enlarged in magnitude. It is only worth noting that within every species the absorption curve shows a peculiar energy dependence. The reasons for this could be further investigated at a lower level to define an even clearer picture of the most harmful particle sources.

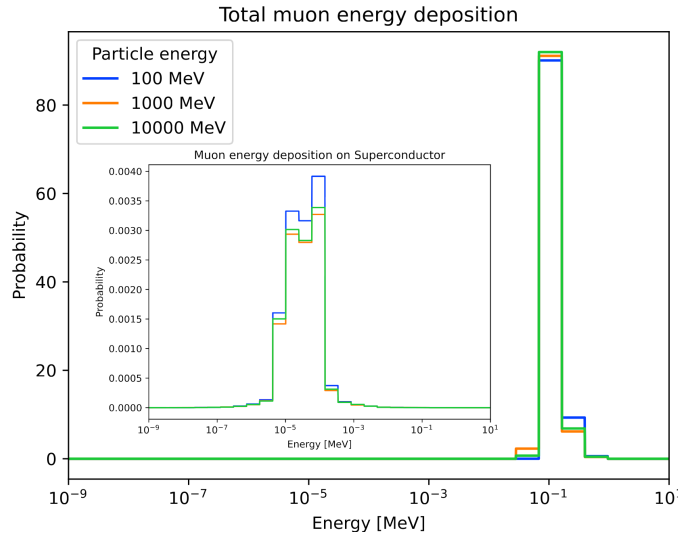

Fig. 8: Energy deposited by muons of different energies (100 MeV in blue, 1 GeV in orange and 10 GeV in green) by direct interaction with the substrate and the superconductor. In the embedded figure a zoom-in of the deposition on the superconductor itself.

B. Deposited energy time persistence and spatial propagation

We further study how the energy deposited by radiation evolves in time and space to understand why the fault persistence in qubits lasts longer than in CMOS and to estimate the probability for a single impinging particle to interact with multiple qubits. Without loss of generality, we study the response to the highest energetic muons tested (10 GeV), considering a sample of 25,000 particles. In any case, for each main result, we also provide an overview of the simulations performed with other particles, showing very similar results.

There is evidence that a radiation-induced error in a superconducting qubit device can last in the order of tens/hundreds of *milliseconds* [2]. This behaviour starkly differs from the classical recovery time of a CMOS (tens of *nanoseconds* [12]). The reasons for this happening are still unclear and partly unknown. Our first aim for this Section is to get a better understanding of the time scales involved in particle-induced energy depositions. In particular, we are concerned with understanding the lifetime of this energy deposition in the Silicon substrate and evaluating at which level the very low temperature at which qubits operate influences the fault persistence.

In Figure 9 we show the energy absorption from the superconducting layer over time. A rapidly decaying amount of energy is deposited on the superconducting portion of the device, peaking at about 1.90 MeV in the first instants after the muon-substrate interaction (*t=0*), and dipping three orders of magnitude after 80 μs. The most significant energy transmission to the superconductor takes place in the first 75 μs since the beginning of the interaction. Nonetheless, it is possible to observe energy depositions on the order of tens of eV for up to 120 μs after the beginning of the interaction, which is still quantitatively relevant in terms of breaking Cooper-pairs,

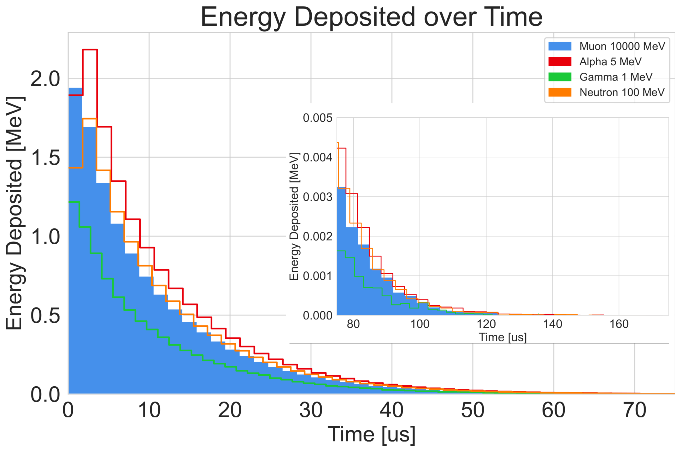

Fig. 9: Energy deposition on the superconductor after phonon absorption over time. Phonons are generated from the interaction of 10 GeV muons with the Silicon substrate of the chip.

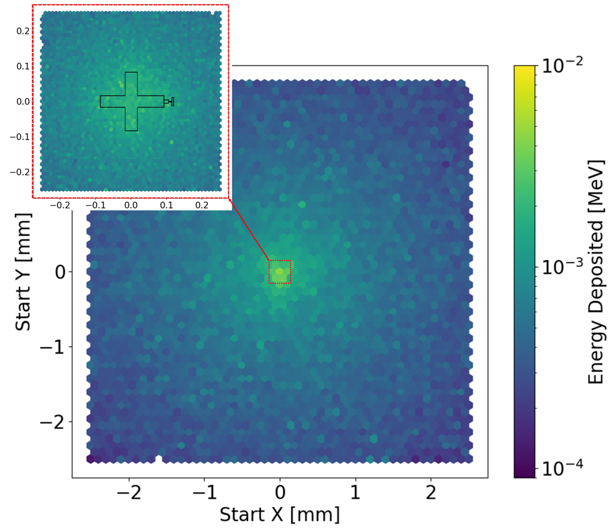

Fig. 10: Energy absorbed by the superconductor with respect to the impact point. Top-down view of the Silicon substrate. The qubit is centred at coordinates (0, 0).

and thus hindering the functioning of a qubit. Following the results in Section IV-E, the amount of energy deposited (i.e., the magnitude of the bars in Figure 9) can be associated with a measure of the probability of modifying the electric state of the superconductor and ultimately the state of the qubit. Our experiment points out that the persistence of the energy within the substrate can not fully justify the millisecond-long error bursts that have been measured [11]. We speculate that phonon-induced effects in the superconductor, namely the breaking of Cooper-pairs, require much longer time to set back to the normal state than phonon interactions in the Silicon substrate. Another important consideration is that the presence of the Copper frame affects the time persistence of the phonon in the substrate [26], [31], [32]. We chose a minimal frame for the system, considering the entire substrate surface, only 1.8% is acoustically coupled to the Copper exit way. To give a clearer picture of the time persistency of the deposited energy in the substrate, we overlapped in Figure 9 the results for other species (100 MeV neutrons, 1 MeV gammas and 5 MeV alphas). They all show the same decaying behaviour and similar persistence over time, thus leading to the same conclusions drawn for muons.

The superconducting component of a qubit is even smaller in terms of area: it covers less than 0.03% of the whole Silicon substrate. Henceforth, it might sound appropriate to search for a *safe distance* from a muon particle impact such that the energy deposition on the qubit will be negligible.

To evaluate the spatial distribution of the charge and estimate the probability for one particle to impact various qubits, we proceed by building a heat map (Figure 10) where we correlate the position of the particle impact with the magnitude of energy deposition on the superconductor (after all the energy transportation processes described). The peak of the deposited energy is generated by those muons hitting the area closest to the qubit, reaching an average energy deposition over time of almost 10 keV. Farther impact points are less prone to lead to an energy deposition on the superconductor, with a lower bound for the average deposited energy on the order of 100 eV. This lower value can be read in relation to the previous one and conveys an indication of a lower probability of energy deposition. Anyway, given the low energy required to break Cooper pairs, it still indicates that there exists no safe radius outer which energy deposition would not affect the superconducting part of the device, or at least this radius is greater than 3.5 mm (maximum distance simulated), which corresponds to 20x superconductor size.

To broaden the results, we performed this experiment with other particle sources. The results for neutrons and gammas show a heatmap almost completely null with few intense (O(100keV) for gammas and O(100keV to 1MeV) for neutrons) dots randomly distributed across all the surface injected. This is in accordance with the experiment done on the SQUID and the energy deposition experiment on the qubit: low probability of depositing energy, but large amounts of energy deposited. For what concerns experiments with alphas, we collected a smaller sample of data. This originates from the fact that their simulation is extremely computationally demanding, since alpha particles are very interacting, making it so that their energy is always completely released on the substrate, creating an even larger number of secondaries, which ends up halting the simulation. What we observed is that every particle impact position led to an intense (O(1-10 MeV)) energy absorption by the superconductor, following the conclusions we drew in the last section. Ultimately, it is interesting to numerically compare the different contributions of various means of energy deposition. We remind that here it has been considered an experiment where 25,000 positive muons hit perpendicularly on a 5 mm x 5 mm surface centred on our qubit model. The total energy deposited on the device is $E_{dep}^{TOT} = 3435 \pm 9$ MeV, and the fraction deposited directly on the sensor is minimal: $E_{dep}^{SUP} = 25.37 \pm 0.03$ keV, which implicitly means that most of it ($> 99.999\%$) is collected on the substrate. A small share ($E_{abs\%}^{SUP} = 0.669\%$) of this energy

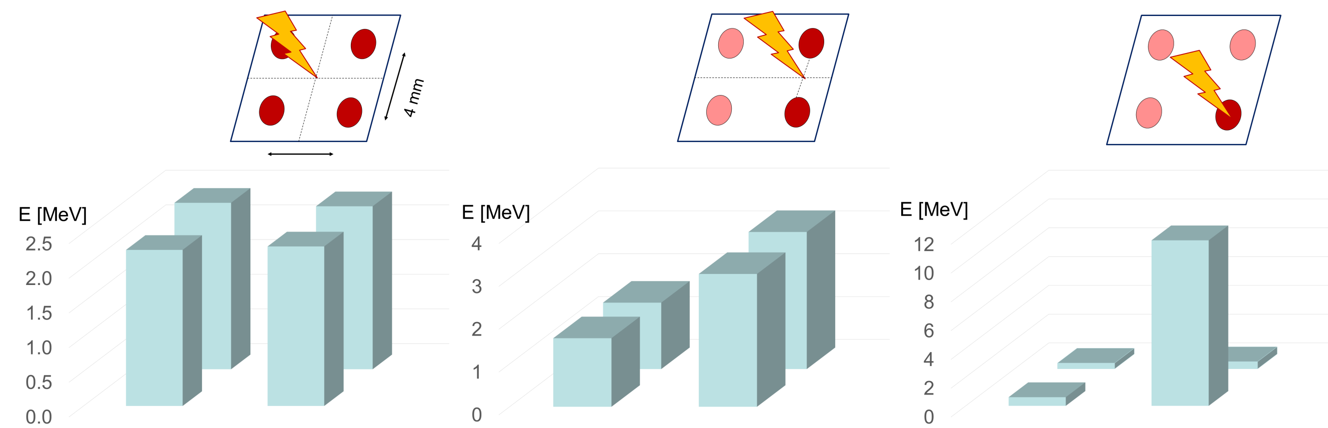

Fig. 11: Energy deposited by 100 MeV positive muons across four qubits on a Silicon substrate. From left to right, the muon generation coordinate changes from the centre of the substrate (equidistant from all qubits), to the midpoint between two qubits, and finally to be centred on one of the four qubits.

amount is then finally absorbed by the superconductor. Despite being a small portion of the total energy deposited, it still counts for an absolute amount of energy of ($E^{SUP}_{abs\%} = 22.98$ MeV, which is $\sim 1000x$ the energy directly deposited on the superconductor.

The last relevant parameter to consider is the number of total phonons absorbed by the superconductor which is $N^{SUP}_{abs} = 1.88 \cdot 10^{10}$. From this, it is straightforward to notice that the average energy absorption per phonon hit is $\langle E^{SUP}_{abs} \rangle = 1.96$ eV. This cross confirms our statements on the harmfulness of far energy depositions and late energy absorptions.

C. Multi qubit corruption

Modern quantum chips contain from a few qubits to hundreds of them. In order to understand the effects of energy diffusion across the Silicon substrate in a multi-qubit setting, we take into consideration a secondary configuration as described in Section III. The goal of this analysis is to detect whether a multi-qubit corruption is possible and, in this case, how likely it is.

We run three separate simulations that differ only by the particle impact coordinate, generating $2,500$ positive muons with an energy of 100 MeV for each one. The first simulation considers the impact point coordinates to be at the centre of the Silicon substrate, equidistant from all the qubits. The second simulation considers the impact point coordinates to be at the middle point between two qubits on the same side of the Silicon substrate. The third simulation picks the impact point coordinates to be those at the centre of one qubit.

In Figure 11 we compare the energy deposition distributions on the four qubits across the three simulations. When injecting on the point equidistant from all qubits, the energy deposition is evenly spread across all of the qubits, peaking at about 2.5 MeV for all of them. The second simulation shows a symmetric imbalance of energy deposition: the two close qubits each absorb about 3 MeV, whilst the two farther qubits both come to absorb less than half of that energy. The last simulation sees more than 12 MeV being absorbed by the qubit lying at the muon generation coordinates. Notably, in this case, we observe that the lifetime of phonons in the Silicon substrate is much lower than that previously commented in Section V-B. This is due to the fact that the proximity of the events to the superconductor makes them more likely to be absorbed in a shorter time span. This only affects the lifespan of secondaries in the substrate, while the total amount of deposited energy is left unaltered.

Ultimately, this confirms that secondary particles diffuse several millimetres through the substrate. Consequently, we infer that particle impacts are likely to generate correlated errors within a quantum system. Therefore, both physical and computer science hardening solutions should consider the probable simultaneous corruptions of qubits.

VI. Conclusions

The most relevant outcome of our analysis is the experimental validation that even extremely light particles are harmful to quantum devices. In particular, given their abundance and interaction rate, muons are the main concern for qubit reliability. They are followed by gamma rays, which contribute massively given their high abundance on earth, and by alpha particles, which, even considering the emission from ultralow-alpha devices, represent an important source of decoherence. In this picture, neutrons only play a minor role in the unreliability of quantum devices.

A second analysis explored the spatial diffusion and temporal persistency of energy in the device substrate. We observe that detrimental energy deposition can happen at every point of the substrate, even far from the superconducting elements. For the tested layout, secondary produced particles lasted in the superconductor for O(100 μs).

Another important outcome of the simulations is the small ratio (1/1000) between direct energy deposition on the superconductor and phonon-induced energy absorption. This shows the importance of addressing hardening solutions which prevent energy diffusion within the substrate. The same conclusion has been drawn by analysing the impacts of particles on a multi-qubit device. The closer a qubit is to the impact point, the higher the energy absorbed. However, in every test, we have also shown that qubits very far from the impact point absorb sufficient energy to be corrupted.

In conclusion, the broad analysis we have presented highlights the threat that radiation poses to quantum computer reliability, and urgently calls for a solution. Our paper provides the foundation meant to guide future research endeavours in this direction by identifying the particles and the mechanisms that should be considered to significantly reduce the fault rate of quantum chips.

References

[1] R. Acharya *et al.*, "Suppressing quantum errors by scaling a surface code logical qubit," *Nature*, vol. 614, no. 7949, pp. 676–681, Feb 2023. [Online]. Available: https://doi.org/10.1038/s41586-022-05434-1

[2] M. McEwen *et al.*, "Resolving catastrophic error bursts from cosmic rays in large arrays of superconducting qubits," *Nature Physics*, vol. 18, no. 1, pp. 107–111, Jan. 2022. [Online]. Available: https://doi.org/10.1038/s41567-021-01432-8

[3] L. Cardani *et al.*, "Reducing the impact of radioactivity on quantum circuits in a deep-underground facility," *Nature Communications*, vol. 12, no. 1, p. 2733, 2021. [Online]. Available: https://doi.org/10.1038/s41467-021-23032-z

[4] ——, "Disentangling the sources of ionizing radiation in superconducting qubits," *The European Physical Journal C*, vol. 83, no. 1, Jan. 2023. [Online]. Available: http://dx.doi.org/10.1140/epjc/s10052-023-11199-2

[5] D. Oliveira *et al.*, "A systematic methodology to compute the quantum vulnerability factors for quantum circuits," 2021.

[6] ——, "Qufi: a quantum fault injector to measure the reliability of qubits and quantum circuits," in *2022 52nd Annual IEEE/IFIP International Conference on Dependable Systems and Networks (DSN)*, 2022, pp. 137–149.

[7] M. Vallero *et al.*, "Understanding logical-shift error propagation in quanvolutional neural networks," *IEEE Transactions on Quantum Engineering*, vol. 5, pp. 1–14, 2024.

[8] ——, "On the efficacy of surface codes in compensating for radiation events in superconducting devices," 2024. [Online]. Available: https://arxiv.org/abs/2407.10841

[9] C. D. Wilen *et al.*, "Correlated charge noise and relaxation errors in superconducting qubits," *Nature*, vol. 594, no. 7863, pp. 369–373, 2021.

[10] J. M. Martinis, "Saving superconducting quantum processors from qubit decay and correlated errors generated by gamma and cosmic rays," *npj Quantum Information*, 2021.

[11] D. Oliveira, E. Auden, and P. Rech, "Atmospheric neutron-induced fault generation and propagation in quantum bits and quantum circuits," *IEEE Transactions on Nuclear Science*, vol. 70, no. 4, pp. 345–353, 2023.

[12] R. Baumann, "Soft errors in advanced computer systems," *IEEE Design Test of Computers*, vol. 22, no. 3, pp. 258–266, May 2005.

[13] Z. K. Minev *et al.*, "Qiskit Metal: An Open-Source Framework for Quantum Device Design & Analysis," 2021. [Online]. Available: https://doi.org/10.5281/zenodo.4618153

[14] M. Kelsey *et al.*, "G4cmp: Condensed matter physics simulation using the geant4 toolkit," *Nuclear Instruments and Methods in Physics Research Section A: Accelerators, Spectrometers, Detectors and Associated Equipment*, vol. 1055, p. 168473, 2023. [Online]. Available: https://www.sciencedirect.com/science/article/pii/S0168900223004631

[15] T. E. Roth, R. Ma, and W. C. Chew, "The transmon qubit for electromagnetics engineers: An introduction," *IEEE Antennas and Propagation Magazine*, vol. 65, no. 2, p. 8–20, Apr. 2023. [Online]. Available: http://dx.doi.org/10.1109/MAP.2022.3176593

[16] G. Catelani *et al.*, "Relaxation and frequency shifts induced by quasiparticles in superconducting qubits," *Phys. Rev. B*, vol. 84, p. 064517, Aug 2011. [Online]. Available: https://link.aps.org/doi/10.1103/PhysRevB.84.064517

[17] Z. Chen *et al.*, "Exponential suppression of bit or phase errors with cyclic error correction," *Nature*, vol. 595, no. 7867, p. 383–387, Jul. 2021. [Online]. Available: http://dx.doi.org/10.1038/s41586-021-03588-y

[18] F. D. Dominicis *et al.*, "Evaluating radiation impact on transmon qubits in above and underground facilities," 2024. [Online]. Available: https://arxiv.org/abs/2405.18355

[19] B. Loer *et al.*, "Abatement of ionizing radiation for superconducting quantum devices," 2024. [Online]. Available: https://arxiv.org/abs/2403.01032

[20] A. P. Vepsäläinen *et al.*, "Impact of ionizing radiation on superconducting qubit coherence," *Nature*, vol. 584, no. 7822, p. 551–556, Aug. 2020. [Online]. Available: http://dx.doi.org/10.1038/s41586-020-2619-8

[21] R. Barends *et al.*, "Coherent josephson qubit suitable for scalable quantum integrated circuits," *Phys. Rev. Lett.*, vol. 111, p. 080502, Aug 2013. [Online]. Available: https://link.aps.org/doi/10.1103/PhysRevLett.111.080502

[22] R. Citro, C. Guarcello, and S. Pagano, "Josephson junctions, superconducting circuits, and qubit for quantum technologies," 2024. [Online]. Available: https://arxiv.org/abs/2405.20911

[23] D. Shen *et al.*, "Character and fabrication of al/al2o3/al tunnel junctions for qubit application," *Chinese Science Bulletin*, vol. 57, no. 4, p. 409–412, Jan. 2012. [Online]. Available: http://dx.doi.org/10.1007/s11434-011-4821-4

[24] W. D. Oliver and P. B. Welander, "Materials in superconducting quantum bits," *MRS bulletin*, vol. 38, no. 10, pp. 816–825, 2013.

[25] M. Kjaergaard *et al.*, "Superconducting qubits: Current state of play," *Annual Review of Condensed Matter Physics*, vol. 11, no. Volume 11, 2020, pp. 369–395, 2020. [Online]. Available: https://www.annualreviews.org/content/journals/10.1146/annurev-conmatphys-031119-050605

[26] E. Yelton *et al.*, "Modeling phonon-mediated quasiparticle poisoning in superconducting qubit arrays," 2024. [Online]. Available: https://arxiv.org/abs/2402.15471

[27] R. Linehan *et al.*, "Estimating the energy threshold of phonon-mediated superconducting qubit detectors operated in an energy-relaxation sensing scheme," 2024. [Online]. Available: https://arxiv.org/abs/2404.04423

[28] T. Sato, "Analytical model for estimating the zenith angle dependence of terrestrial cosmic ray fluxes," *PLOS ONE*, vol. 11, no. 8, pp. 1–22, 08 2016. [Online]. Available: https://doi.org/10.1371/journal.pone.0160390

[29] S. B. Kaplan, "Acoustic matching of superconducting films to substrates," *Journal of Low Temperature Physics*, vol. 37, no. 3–4, p. 343–365, Nov. 1979. [Online]. Available: http://dx.doi.org/10.1007/BF00119193

[30] J. F. Ziegler and H. Puchner, *SER–history, Trends and Challenges: A Guide for Designing with Memory ICs*. Cypress, 2010.

[31] V. Iaia *et al.*, "Phonon downconversion to suppress correlated errors in superconducting qubits," *Nature Communications*, vol. 13, no. 1, Oct. 2022. [Online]. Available: http://dx.doi.org/10.1038/s41467-022-33997-0

[32] A. Bargerbos *et al.*, "Mitigation of quasiparticle loss in superconducting qubits by phonon scattering," *Physical Review Applied*, vol. 19, no. 2, Feb. 2023. [Online]. Available: http://dx.doi.org/10.1103/PhysRevApplied.19.024014